IEEE Open Journal of
Vehicular Technology

Received 26 June 2020; accepted 21 July 2020. Date of publication 30 July 2020;
date of current version 14 August 2020. The review of this article was coordinated by Editor S. Sun.

Digital Object Identifier 10.1109/OJVT.2020.3013149

Vehicle Lateral Dynamic Identification Method Based on Adaptive Algorithm

ANTÓNIO LOPES (Student Member, IEEE), AND RUI ESTEVES ARAÚJO (Member, IEEE)

INESC TEC and the Department of Electrical and Computer Engineering, Faculty of Engineering, University of Porto, 4200-465 Porto, Portugal

CORRESPONDING AUTHOR: ANTÓNIO LOPES (e-mail: antonio.lopes@fe.up.pt)

This work was supported by Fundação para a Ciência e Tecnologia (FCT) under Grant SFRH/BD/116523/2016.

ABSTRACT The development of advanced driver assistance systems relies on an accurate estimation of the tire-road friction coefficient and cornering stiffness of the vehicle, which are closely linked to internal and external driving conditions. In this paper, an identification algorithm capable of simultaneously estimate the friction coefficient and cornering stiffness of the front and rear tires is pursued. A nonlinear adaptive law is proposed for the estimation of vehicle parameters under certain excitation conditions. It is shown that, by exploring the lateral dynamic of the vehicle, the convergence of the parameters to their true values can be guaranteed. A comprehensive study has been carried out in order to reveal the necessary conditions for convergence and observability of the parameters. Simulation results with a high fidelity full order Carsim model show a good performance of the proposed identification method.

INDEX TERMS Adaptive estimation, parameter estimation, system identification, vehicle dynamics.

I. INTRODUCTION

Over the past few decades, there has been an increasing interest in academic as well as industrial research to develop advanced driver assistance systems, that aim to further improve the overall safety, comfort and efficiency of the road vehicle. The combination of sensor information, estimation of internal and external conditions and advanced control methods have enable the development of driver assistant systems that improve the maneuverability of the vehicle, even in challenging driving conditions, thus achieving a high level of comfort and road safety [1]–[4].

One of the most challenging problems in vehicle dynamics is the external driving conditions that a vehicle may encounter during its operation. Advanced driver assistance systems such as: electronic stability control (ESC), anti-lock braking system (ABS), adaptive cruise control (ACC) and collision avoidance aim to minimize the effect of these external conditions. According to [2], [3], [5]–[7] an accurate estimation of vehicle states and/or parameters is required to obtain an effective performance of the driver assistance systems. Even though some states of the system are of paramount importance, in practice, such variables may be difficult or even impossible to be directly measured. Nonetheless, in order to pursue a road adaptive control methodology, some authors have proposed estimation techniques that aims to obtain a reliable estimate of road and vehicle parameters such as tire-road friction coefficient, cornering stiffness, side slip angle, lateral forces, etc [2]–[11].

As the automation level in vehicle systems increases, there will be a growing need for more reliable and safe systems. Vehicle active safety system will be able to monitor different aspects of the vehicular system, among them the road condition. This information will become available to other vehicles through vehicle-2-vehicle (V2V) communication, allowing this information to be broadcast. Challenging road conditions resulting from oil spillage, snowy conditions or other abnormal conditions that may change the friction coefficient of the road can be reported, allowing other vehicles to become aware of this situation and take preventive actions, e.g. reduce the speed of the vehicle, reconfigure controller scheme, etc [12], [13].

The tire-road friction coefficient is one of the most widely investigated external parameter of the ground vehicle system and many authors have pursued different approaches by analysing the lateral and/or longitudinal dynamics of the vehicle. In [14] and [9] a real-time estimation of such

coefficient is proposed by estimating the wheel slip value, which corresponds to the peak–value of the tire-road friction curve. In [10] a sensor fusion method is proposed for the estimation of the friction coefficient by introducing a complementary filter with certainty factors that weights the estimated friction coefficient through the vehicle characteristic and the estimated longitudinal road frictions under ABS and ESC.

A wide spread vehicle dynamic model-based estimation approach has been pursued through filter-based methodology, which is typically formulated by Kalman filter theory [8]. In [15], an algorithm combining an auxiliary particle filter (PF) and an extended Kalman filter (EKF) is developed to estimate the tire-road friction coefficient, in real time, in the presence of strong nonlinearity and non-Gaussian noise. The auxiliary PF is able to filter the non-Gaussian noise, thus obtaining a side slip angle estimation, the iterative EKF is then pursued to optimize the result. A Kalman filter is also proposed in [6] to achieve an accurate side slip angle estimation by investigating both kinematics and dynamics vehicle models.

A different approach can be found in [4], where the authors develop three observers for the estimation of slip ratios and longitudinal tire forces, this information is used to identify the friction coefficient through recursive least-squares parameter identification. Others observer-based least square identification methods, that investigates the estimation of tire-road friction coefficient, can be found in [16]–[18]. A sensor oriented approach was pursued in [19], [20]. In [19] the friction coefficient estimation is based on signals extracted directly from tire sensors. Although this methodology provides good estimation of both slip angle and tire-road friction coefficient, it requires the installation and calibration of additional sensors in the system.

A robust estimation design of friction coefficient is pursued in [12] by constructing four estimate methods based on four different excitation conditions. These four methods are integrated to allow an extended working range of the estimator and thus improve its robustness. A robust estimation algorithm is also presented in [13] based on the lateral dynamic of the system. Nonetheless, the quality of the estimation depends on the persistent excitation of the system and the richness of such excitation [13]. Other robust methodologies were also developed for the estimation of the tire-road friction coefficient, in [21] a framework is developed by adopting a novel strategy, that is based on the estimation of the front axle lateral force, combined with an indirect measurement of the total aligning torque and the lateral force acting in the front axle. A nonlinear adaptive observer is then designed to estimate the tire-road friction coefficient with guaranteed stability properties.

Some authors have pursued a simultaneous estimation of tire-road friction coefficient and the cornering stiffness of the system [2], [22]. In [2] the authors pursue an identification algorithm based on an adaptive gradient algorithm to obtain a simultaneous estimation of the friction coefficient and the front tire cornering stiffness coefficient. A sequential identification algorithm is proposed in [22]. The estimation of the cornering stiffness coefficient is first obtained with negligible lateral dynamic by exciting the system with an additional yaw moment. Once the estimation of the cornering stiffness is obtained the friction coefficient estimator is enabled whenever the vehicle performs a turning maneuver.

Although several different approaches have been developed, in the current literature, for the identification of driving conditions of the ground vehicle system, there has been a lack of investigation of the necessary excitation conditions for the estimation of the vehicle parameters. The investigation presented in this paper will be based, exclusively, on the lateral dynamic of the vehicle. A Lyapunov based adaptive law will be introduced for the estimation of the aforementioned parameters and the convergence of the proposed law will be analyzed. The main contributions of this paper are summarized as follows:

1) Development of a sequential two stage adaptive algorithm for the simultaneous identification of the tire-road friction and cornering stiffness coefficient of both front and rear tires;
2) A novel observer-based adaptation law is proposed for the vehicle system and its convergence is demonstrated through Lyapunov theory;
3) To verify in detail the persistent excitation and distinguishability properties of the model parameters, a geometric analysis of Lyapunov function was made to guarantee the convergence of parameters is well founded.

The rest of the paper is organized as follows. The vehicle lateral dynamic model is investigated in Section II. The developed identification algorithm and the associated adaptive laws are explored in Section III. The convergence of the proposed solution is analyzed in Section IV. Finally, simulations results, carried out in a high fidelity CarSim model, are presented in Section V, followed by the conclusions in Section VI.

II. VEHICLE LATERAL DYNAMIC MODEL

The ground vehicle planar dynamic model will be pursued by exploring the *Newton-Euler* equations of motion [23]:

$$\Sigma = \begin{cases} \dot{v}_x = \frac{1}{m}(F_x) + \dot{\psi} v_y & \text{(1a)} \\ \dot{v}_y = \frac{1}{m}(F_{yr} + F_{yf}) - \dot{\psi} v_x & \text{(1b)} \\ \ddot{\psi} = \frac{1}{I_z}(l_f F_{yf} - l_r F_{yr}) & \text{(1c)} \end{cases}$$

where v_x and v_y are the longitudinal and lateral components of the vehicle velocity v, ψ is the yaw angle of the vehicle, m denote the mass of the vehicle, I_z is the moment of inertia of the system and l_f and l_r are the distance from the center of gravity (CoG) to the front and rear tires, respectively. The longitudinal forces acting on the vehicle are defined by $F_x = F_{xf} + F_{xr}$ and the lateral forces applied to the front and rear tires are expressed as F_{yf} and F_{yr}, respectively (see Fig. 1).

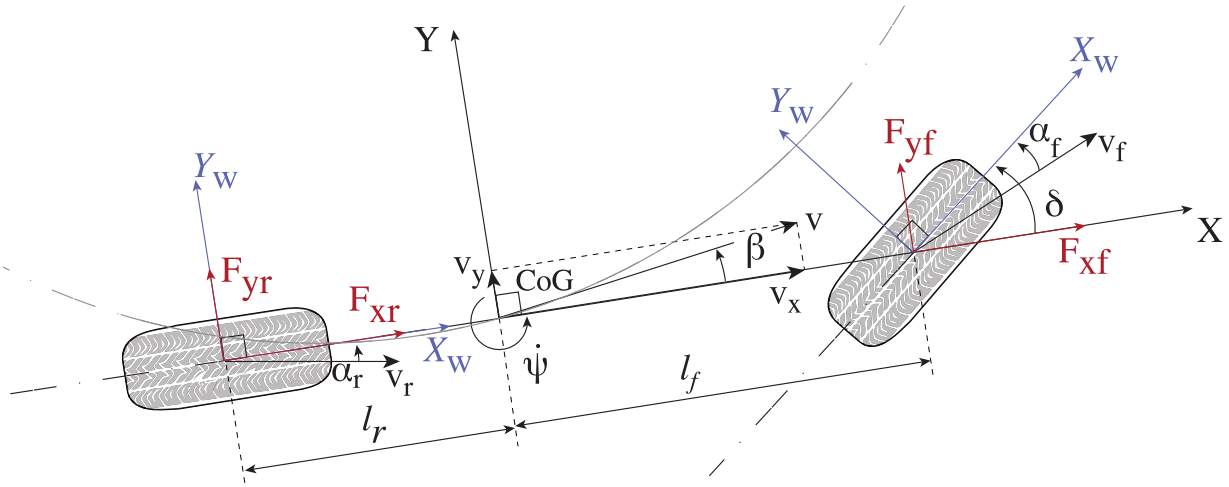

FIGURE 1. Single-track model diagram for lateral vehicle dynamics. Forces and angles applied to the front (left) and rear (right) wheel (vehicle axis expressed by $X - Y$ and wheel axis expressed by $X_W - Y_W$).

The rigid vehicle model in (1) neglects the vertical dynamic introduced by the suspension system, thus assuming an equal force distribution on the left and right tires. This simplification allow us to deal with the vehicle system as a single-track (bicycle) model presented in Fig. 1 [23].

To provide a decouple analysis of the lateral dynamics with respect to the longitudinal dynamics of the vehicle, it will be assumed that the longitudinal velocity is a known disturbance of the system and the vehicle yaw rate and lateral velocity are available, resulting the following lateral model:

$$\Omega = \begin{cases} \dot{v}_y = \frac{1}{m}(F_{yr} + F_{yf}) - \dot{\psi} v_x & \text{(2a)} \\ \ddot{\psi} = \frac{1}{I_z}(l_f F_{yf} - l_r F_{yr}) & \text{(2b)} \end{cases}$$

A. LATERAL FORCES

The lateral forces, depicted in Fig. 1, have a nonlinear characteristic that varies with: the tire side slip angle α, the normal forces applied on the tires F_z and the road conditions defined by the friction coefficient μ [1]–[3]. Fig. 1 presents the forces acting on the front and rear tire, as well as the angles of the tires in a cornering maneuver, with a steering angle δ.

According to [1]–[3], [12], [13], by assuming a small longitudinal slip, the tire lateral force can be expressed by the following mathematical model (Brush tire model):

$$F_{yi} = 2\left(C_i\phi_i - \frac{C_i^2}{\mu}\phi_i\gamma_i + \frac{1}{3}\frac{C_i^3}{\mu^2}\phi_i\gamma_i^2\right), \qquad (3)$$

if $|\frac{C_i \tan(\alpha_i)}{\mu F_{zi}}| \leq 3$, with

$$\phi_i = \tan(\alpha_i), \qquad \gamma_i = \frac{1}{3}\frac{|\tan(\alpha_i)|}{F_{zi}},$$

where the subscript i defines the rear r and front f tire. The front and rear tire slip angle (α_f and α_r respectively) are presented in Fig. 1 and can be estimated according to [1]–[3]. The normal forces that act on the front F_{zf} and rear F_{zr} tires can be estimated by [3], [22]:

$$F_{zf} = \frac{mgl_r - m\dot{v}_x h}{l_r + l_f}, \qquad F_{zr} = \frac{mgl_f + m\dot{v}_x h}{l_r + l_f}, \qquad (4)$$

where g is the gravitational acceleration (9.81 m/s^2) and h is the height of the vehicle *CoG*.

III. IDENTIFICATION ALGORITHM

The developed algorithm is based on a two stage adaptive methodology depicted in Fig. 2. The convergence of the proposed adaptive law will be addressed through Lyapunov theory.

The proposed adaptive algorithm will be developed as a sequential two stage mechanism. In the first stage, an adaptive algorithm is projected to identify the front cornering stiffness as well as the friction coefficient of the system. Once these parameters are obtained, a trigger mechanism enables the second layer that will produce an estimate of the rear cornering stiffness. The estimated lateral forces are then expressed according to the estimated parameters and the calculated vertical forces of the system.

The stability analysis of the adaptive system will be pursued by studying the error model, which represents the dynamic relationship between the parametric error and an unknown tuning error that is adjusted by the former [24], [25].

Let us assume an unknown constant vector $\hat{\theta}$, such that, the output of the adaptive system follows the output of the reference model when $\theta(t) \equiv \hat{\theta}$. Furthermore, let the state error vector $e(t)$ and the parameter error vector $\tilde{\theta}(t)$ be defined as:

$$e(t) \triangleq x(t) - \hat{x}(t), \quad \tilde{\theta} \triangleq \theta(t) - \hat{\theta}, \qquad (5)$$

where $\hat{x}$ is the estimated state trajectory and θ is the parameter vector. We will be interested in pursuing a zero state error $e(t)$

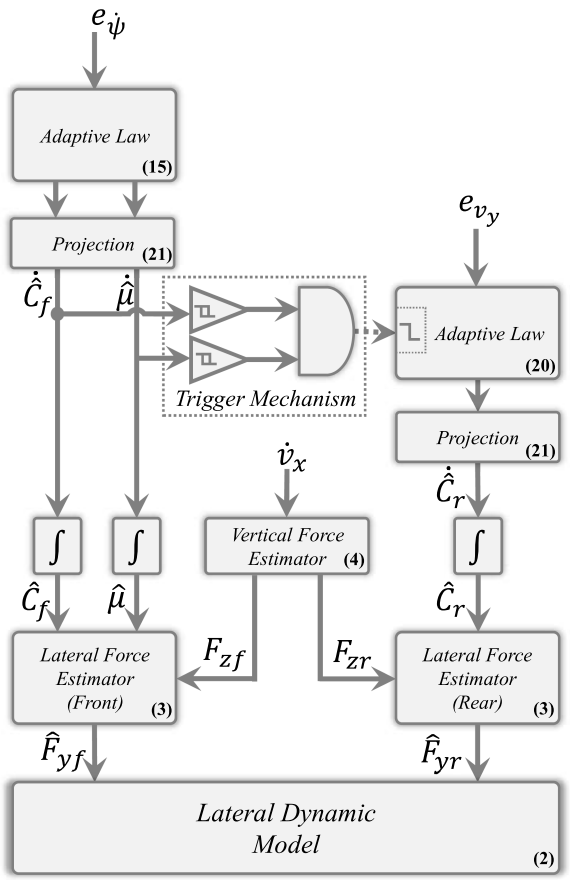

FIGURE 2. Proposed two-stage adaptive algorithm for vehicle parameter identification.

as $t \longrightarrow \infty$ as well as $lim_{t\longrightarrow\infty}\tilde{\theta}(t) = 0$, in the absence of external disturbances [24], [25].

A. ADAPTIVE LAWS

Let us consider the system (Ω) in (2) and let the error state vector e and the parameter error vector $\tilde{\theta}$ be expressed as:

$$e = \begin{bmatrix} e_{\dot\psi} \\ e_{v_y} \end{bmatrix} = \begin{bmatrix} \dot\psi - \dot{\hat\psi} \\ v_y - \hat{v}_y \end{bmatrix}, \quad \tilde{\theta} = \begin{bmatrix} \tilde{C}_f \\ \tilde{\mu} \\ \tilde{C}_r \end{bmatrix} = \begin{bmatrix} C_f - \hat{C}_f \\ \mu - \hat{\mu} \\ C_r - \hat{C}_r \end{bmatrix}, \tag{6}$$

A Lyapunov function will be chosen as follows:

$$\begin{aligned} V &= \frac{1}{2}\left(ee^T + \tilde{\theta}\tilde{\theta}^T\right), \\ &= \frac{1}{2}\left(\underbrace{e_{\dot\psi}^2 + \tilde{C}_f^2 + \tilde{\mu}^2}_{V_1} + \underbrace{e_{v_y}^2 + \tilde{C}_r^2}_{V_2}\right). \end{aligned} \tag{7}$$

For the sake of simplicity, the analysis of the previous Lyapunov function will be addressed by studying the functions V_1 and V_2 separately.

Let us first investigate the V_1 function defined as:

$$V_1 = \frac{1}{2}e_{\dot\psi}^2 + \frac{1}{2}\tilde{C}_f^2 + \frac{1}{2}\tilde{\mu}^2, \tag{8}$$

By differentiating the expression in (8) follows:

$$\begin{aligned} \dot{V}_1 &= e_{\dot\psi}\dot{e}_{\dot\psi} + \tilde{C}_f\dot{\tilde{C}}_f + \tilde{\mu}\dot{\tilde{\mu}}, \\ &= e_{\dot\psi}(\ddot\psi - \ddot{\hat\psi}) + \tilde{C}_f\dot{\tilde{C}}_f + \tilde{\mu}\dot{\tilde{\mu}}, \\ &= e_{\dot\psi}\left[f_{\dot\psi}(\theta,\alpha) - \left(\hat{f}_{\dot\psi}(\hat\theta,\alpha) + l_1 e_{\dot\psi}\right)\right] + \tilde{C}_f\dot{\tilde{C}}_f + \tilde{\mu}\dot{\tilde{\mu}}, \end{aligned} \tag{9}$$

where $f_{\dot\psi}(\theta,\alpha)$ is defined as in (2b), $\hat{f}_{\dot\psi}(\hat\theta,\alpha)$ is the estimation of the previous function and $l_1 e_{\dot\psi}$ is an observer term, with l_1 expressing the observer gain.

According to the representation of the system (Ω) in (2), the lateral force of the rear tire can be expressed as function of the lateral force of the front tire as follows [2]:

$$F_{yr} = m\dot\psi v_x + m\dot{v}_y - F_{yf}, \tag{10}$$

The yaw rate can now be expressed exclusively as a function of the lateral force of the front tire as:

$$f_{\dot\psi}(\theta,\alpha) = \frac{1}{I_z}\left((l_f + l_r)F_{yf} - l_r m\dot\psi v_x - l_r m\dot{v}_y\right), \tag{11}$$

By replacing the function (11) in (9) results:

$$\begin{aligned} \dot{V}_1 = e_{\dot\psi}\Bigg(&\frac{1}{I_z}\left((l_f + l_r)F_{yf}\right) - \frac{1}{I_z}\left((l_f + l_r)\hat{F}_{yf}\right) - l_1 e_{\dot\psi} \\ &- \frac{l_r}{I_z}mv_x(\dot\psi - \dot{\hat\psi})\Bigg) + \tilde{C}_f\dot{\tilde{C}}_f + \tilde{\mu}\dot{\tilde{\mu}}, \\ = e_{\dot\psi}&\frac{(l_f + l_r)}{I_z}\left(F_{yf} - \hat{F}_{yf}\right) - \frac{l_r}{I_z}mv_x e_{\dot\psi}^2 - l_1 e_{\dot\psi}^2 \\ &+ \tilde{C}_f\dot{\tilde{C}}_f + \tilde{\mu}\dot{\tilde{\mu}}. \end{aligned} \tag{12}$$

We will now pursue a parameter oriented representation by introducing the tire nonlinear dynamic presented in (3) in the previous analysis, resulting:

$$\begin{aligned} \dot{V}_1 = e_{\dot\psi}&\frac{2(l_f + l_r)}{I_z}\Bigg(C_f\phi_f - \frac{C_f^2}{\mu}\phi_f\gamma_f + \frac{1}{3}\frac{C_f^3}{\mu^2}\phi_f\gamma_f^2 \\ &- \hat{C}_f\phi_f + \frac{\hat{C}_f^2}{\hat\mu}\phi_f\gamma_f - \frac{1}{3}\frac{\hat{C}_f^3}{\hat\mu^2}\phi_f\gamma_f^2\Bigg) \\ &+ \tilde{C}_f\dot{\tilde{C}}_f + \tilde{\mu}\dot{\tilde{\mu}} - \frac{l_r}{I_z}mv_x e_{\dot\psi}^2 - l_1 e_{\dot\psi}^2, \end{aligned} \tag{13}$$

After some straightforward algebraic manipulation:

$$\begin{aligned} \dot{V}_1 = \tilde{C}_f&\left[\frac{2\phi_f(l_f + l_r)}{I_z}g_f(\hat{C}_f,\mu,C_f,\alpha_f)e_{\dot\psi}\right] \\ &+ \tilde{\mu}\left[\frac{2\phi_f\gamma_f\hat{C}_f(l_f + l_r)}{\hat\mu I_z}h_f(\hat\mu,\hat{C}_f,\mu,C_f,\alpha_f)e_{\dot\psi}\right] \\ &+ \tilde{C}_f\dot{\tilde{C}}_f + \tilde{\mu}\dot{\tilde{\mu}} - l_1 e_{\dot\psi}^2 - \frac{l_r}{I_z}mv_x e_{\dot\psi}^2, \end{aligned} \tag{14}$$

with,

$$g_i(\hat{C}_i,\mu,C_i,\alpha_i)=\left[1-\frac{(C_i+\hat{C}_i)\gamma_i}{\mu}+\frac{(C_i^2+\hat{C}_i^2+C_i\hat{C}_i)\gamma_i^2}{3\mu^2}\right],$$

$$h_i(\hat{\mu},\hat{C}_i,\mu,C_i,\alpha_i)=\left[\frac{1}{\mu}-\frac{\hat{C}_i^2(\hat{\mu}+\mu)\gamma_i}{\hat{\mu}\mu}\right].$$

Assumption 1 (Projection): The estimated tire-road friction coefficient will be bounded by the set $\hat{\mu},\mu\in\mathcal{U}$ and tire cornering stiffness will be bounded by $\hat{C}_i,C_i\in\mathcal{C}$, as the system will not be defined outside these sets. This constraint will be guaranteed by the projection operator presented later in this paper [24], [26].

The previous assumption implies that the functions $g_f(\hat{C}_f,\mu,C_f,\alpha_f)$ and $h_f(\hat{\mu},\hat{C}_f,\mu,C_f,\alpha_f)$ can also be bounded [24]. Let $\zeta > g_f(\hat{C}_f,\mu,C_f,\alpha_f)$ and $\lambda > h_f(\hat{\mu},\hat{C}_f,\mu,C_f,\alpha_f)\quad\forall\quad\hat{\mu}\in\mathcal{U},\hat{C}_f\in\mathcal{C},\mu\in\mathcal{U},C_f\in\mathcal{C},\alpha_f\in\mathcal{A}$, then it is possible to define the following adaptive law:

$$\dot{\hat{C}}_f = -\frac{2\zeta\phi_f(l_f+l_r)}{I_z}e_{\dot{\psi}}, \tag{15a}$$

$$\dot{\hat{\mu}} = -\frac{2\lambda(l_f+l_r)\phi_f\gamma_f\hat{C}_f}{\hat{\mu}I_z}e_{\dot{\psi}}. \tag{15b}$$

The adaptive law in (15) guarantees the convergence of the parameters in the steady state condition ($\dot{C}_f\approx 0$ and $\dot{\mu}\approx 0$). The observer gain l_1 will be defined as a positive constant that will be designed to minimize the "bursting" phenomena, usually associated to nonlinear adaptive laws [26], [27].

Similarly to what was done for the first term of the proposed Lyapunov function, we will now investigate V_2 given by:

$$V_2=\frac{1}{2}e_{v_y}^2+\frac{1}{2}\tilde{C}_r^2, \tag{16}$$

Differentiating the previous function:

$$\begin{aligned}\dot{V}_2 &= e_{v_y}\dot{e}_{v_y}+\tilde{C}_r\dot{\tilde{C}}_r,\\ &= e_{v_y}(\dot{v}_y-\dot{\hat{v}}_y)+\tilde{C}_r\dot{\tilde{C}}_r,\\ &= e_{v_y}\left(f_{v_y}(\theta,\alpha)-(\hat{f}_{v_y}(\hat{\theta},\alpha)+l_2e_{v_y})\right)+\tilde{C}_r\dot{\tilde{C}}_r\end{aligned} \tag{17}$$

where $f_{v_y}(\theta,\alpha)$ expresses the vehicle lateral velocity model presented in (2a) and $\hat{f}_{v_y}(\hat{\theta},\alpha)$ is the estimation of the function. Once again, an observer term $l_2e_{v_y}$ is introduced, with l_2 defining the observer gain. By replacing (2a) in (17) arise the following expression:

$$\dot{V}_2=e_{v_y}\left(\frac{1}{m}(F_{yr}-\hat{F}_{yr})+\frac{1}{m}(F_{yf}-\hat{F}_{yf})\right)-l_2e_{v_y}^2+\tilde{C}_r\dot{\tilde{C}}_r, \tag{18}$$

Assumption 2 (Parameter Convergence): The proposed two stage adaptive algorithm is a sequential mechanism, as a result, the lateral velocity estimator will be activated only if the previous adaptive law converges to a steady state value. Furthermore, it will be assumed that the vehicle is persistently excited, such that, the parameters $\hat{C}_f$ and $\hat{\mu}$ converge to its true values. This assumption will be challenged later in this paper, but, for the purpose of this discussion, we will assume that $\hat{F}_{yf}$ converges to F_{yf}.

By considering the previous assumption:

$$\dot{V}_2=e_{v_y}\left(\frac{1}{m}(F_{yr}-\hat{F}_{yr})\right)-l_2e_{v_y}^2+\tilde{C}_r\dot{\tilde{C}}_r.$$

After replacing the tire nonlinear model given by (3):

$$\begin{aligned}\dot{V}_2 &= \frac{e_{v_y}}{m}2\Bigg(C_r\phi_r-\frac{C_r^2}{\mu}\phi_r\gamma_r+\frac{1}{3}\frac{C_r^3}{\mu^2}\phi_r\gamma_r^2\\ &\quad-\hat{C}_r\phi_r+\frac{\hat{C}_r^2}{\hat{\mu}}\phi_r\gamma_r-\frac{1}{3}\frac{\hat{C}_r^3}{\hat{\mu}^2}\phi_r\gamma_r^2\Bigg)+\tilde{C}_r\dot{\tilde{C}}_r-l_2e_{v_y}^2,\\ &= \tilde{C}_r2\left[\phi_rg_r(\hat{C}_r,\mu,C_r,\alpha_r)\frac{e_{v_y}}{m}\right]+\tilde{C}_r\dot{\tilde{C}}_r-l_2e_{v_y}^2.\end{aligned} \tag{19}$$

The adaptation law is design to achieve $\dot{V}_2\leq 0$ by defining:

$$\dot{\hat{C}}_r=-\frac{2\zeta\phi_r}{m}e_{v_y}, \tag{20}$$

and by designing an observer gain $l_2>0$.

B. PROJECTION OPERATOR

The proposed adaptive laws (15) and (20) allow the estimated parameters to take any value in $\mathbb{R}$. However, the estimated variables represent the parameters of a physical system, from which we may have some *a priori* knowledge as to where these parameters are located in $\mathbb{R}$ [26].

Since the desired parameters of the system can be bounded by some arbitrary values we may use this information to design adaptive laws that constraint their search to a given set (see Assumption 1), such procedure will reduce large transients and potentially speed up the convergence of the parameters [26].

Another relevant aspect of pursuing an adaptive law with projection operator is related to the ability to bound the functions $g_i(\hat{\mu},\hat{C}_i,\mu,C_i,\alpha_i)$ and $h_i(\hat{\mu},\hat{C}_i,\mu,C_i,\alpha_i)$, which are required to have this property in order to prove convergence of the proposed adaptive law.

For the aforementioned reasons, the following projection strategy will be pursued [24]:

$$\dot{\tilde{\theta}}=\Gamma-\kappa(\tilde{\theta}-\bar{\theta}),\quad \kappa>0,$$

$$\bar{\theta}=\begin{cases}\tilde{\theta}, & \tilde{\theta}\in\Theta\\ \theta_{\max}, & \tilde{\theta}>\theta_{\max}\\ \theta_{\min}, & \tilde{\theta}<\theta_{\min}\end{cases} \tag{21}$$

where Γ is the adaptive law defined in (15) and (20), and $\theta_{\max}$ and $\theta_{\min}$ are respectively the maximum and minimum value that θ can take in the set Θ. To account for the projection term, the Lyapunov function candidate can be modified following the results in [28].

C. TRIGGER MECHANISM

The adaptive law presented in (20) is based on Assumption 2, that the first adaptive laws (15a) and (15b) have converged to their true values, thus obtaining an estimate of the lateral force of the front tires ($\hat{F}_{yf} \approx F_{yf}$).

As depicted in Fig. 2, the trigger mechanism will rely on the output of the first level adaptive laws to ensure that the second level will be activated whenever the convergence of the front cornering stiffness and the friction coefficient is achieved. When the adaptive laws (15) goes to zero we will consider that the true values of the parameters are obtained and the second stage of the proposed sequential algorithm can be activated. To prevent any chattering effect in the second level of the developed algorithm, a Schmitt trigger will be implemented for the trigger mechanism.

IV. CONVERGENCE ANALYSIS

Until this point, we have consider that the vehicle is somehow persistently excited and, as a result, the adaptive laws presented in Section III leads the estimated parameters ($\hat{C}_f$, $\hat{C}_r$ and $\hat{\mu}$) to their true values (see Assumption 2).

The concept of persistent excitation is extremely relevant in the context of system identification. This property of the system is crucial in adaptive systems where the convergence of the parameters is the main objective. The estimated parameters will converge exponentially fast if the reference input is chosen to be sufficiently rich so that the signal information vector is persistently excited over an interval [29], [30].

Definition 1 (Persistent Excitation [30]): A bounded function $x : [0, \infty) \longrightarrow \mathbb{R}^n$ is said to be *persistently excited* with a level of excitation $\eta > 0$ if there exists $T_0 \in \mathbb{R}^+$ such that:

$$\int_t^{t+T_0} x(\tau)x^T(\tau)d\tau \geq \eta T_0 I, \quad \forall t \geq 0$$

Due to the nonlinear characteristic of the tires, we may encounter situations where the parameters of the system may converge to incorrect values, as it may be driven, by the adaptive law, to an indistinguishable state of the nonlinear system. The concept of indistinguishability is directly related to observability of nonlinear system [31] and is defined next.

Definition 2 (Indistinguishable Points [31]): A pair of points x^1 and x^2 are said to be indistinguishable if (Ω, x^1) and (Ω, x^2) realize the same input-output map, i.e., for every admissible input $(u(t), [t^1, t^2])$,

$$\Omega_{x_1}(u(t), [t^1, t^2]) = \Omega_{x_2}(u(t), [t^1, t^2]).$$

Definition 1 and definition 2 address the necessary conditions for convergence and observability of the estimated parameters, respectively. Note that, some authors have presented the distinguishability property as "richness" of the excitation [13], [30]. From an engineering point of view, it is understandable that, if a vehicle follows in a straight line with no lateral dynamic, the vehicle will not produce a lateral motion resulting in an unobservable system [13].

A. GEOMETRIC ANALYSIS

In order to obtain a more meaningful understanding of the vehicle lateral dynamic and the effect of the nonlinear tire-road characteristic, we will now pursue a geometric analysis of the set in which the adaptive algorithm will converge.

We will initially analyze the first adaptive law by exploring the proposed Lyapunov function (8). The square of the yaw rate error is represented in Fig. 3 for different estimated parameters ($\hat{\mu}$ and $\hat{C}_f$). To ensure a more insightful description, the real parameters of the system will be fixed to arbitrary values, allowing a decouple analysis of the estimated parameters.

The results from Fig. 3(a) to Fig. 3(d) explore different tire slip angles α_f of the front tire. From the previous results, it is straightforward that the square of the yaw rate error does not present an unique global minimum in any situation presented in Fig. 3. This factor lead us to conclude that, although a minimum value can be reached, there is no guarantee that the estimated parameters converge to their true values.

Note that, no estimation can be obtained if there is no lateral dynamic in the vehicle i.e if there is no persistent excitation in the system ($\alpha_f \approx 0$). Nonetheless, even if parameter convergence is achieved by ensuring the persistent excitation of the vehicle, the convergence of the parameters to its true values cannot be guaranteed. By analysing Fig. 3 becomes clear that a zero error can be attained by different points $x^1 = [\hat{C}_f^1, \hat{\mu}^1], \ldots, x^n = [\hat{C}_f^n, \hat{\mu}^n]$ making it impossible to distinguish between the true values and other possible parameter values i.e. there exists n indistinguishable points if we introduce a constant tire slip angle ($\alpha_f(t) = a$).

To address the indistinguishability property, we will now investigate an input $\alpha_f(t)$ that may command the system to a set in which only one parameter pair $[\hat{C}_f, \hat{\mu}]$ can be attained. By imposing an arbitrary function to the system input $\alpha_f(t)$ we aim to achieve a distinguishable parameter pair, thus ensuring the convergence of the parameters estimation to its true values.

Let the tire slip angle input be a smooth (class C^∞) periodic function defined by:

$$\alpha_f(t) = a \sin(\omega t), \tag{22}$$

with a expressing the signal amplitude and ω the angular frequency, then, the system will evolve from the set presented in Fig. 3(a) to the set presented in Fig. 3(d) periodically. This sinusoidal function will enforce a given trajectory to the estimated parameters which will be designed to ensure that those values converge to a distinguishable set, where only a pair $[\hat{C}_f, \hat{\mu}]$ is valid for all t. Note that, a sinusoidal signal with period $T = 1/\omega$ will have at most T distinct frequencies in the spectrum, thus it is persistently exciting of, at most, order T. A more detailed discussion over the advantages and disadvantages of periodic inputs for the purpose of system identification can be found in [32].

The proposed periodic function in (22) has two design parameters, a and ω, that represent, respectively, the amplitude and frequency of the sinusoidal function. These two

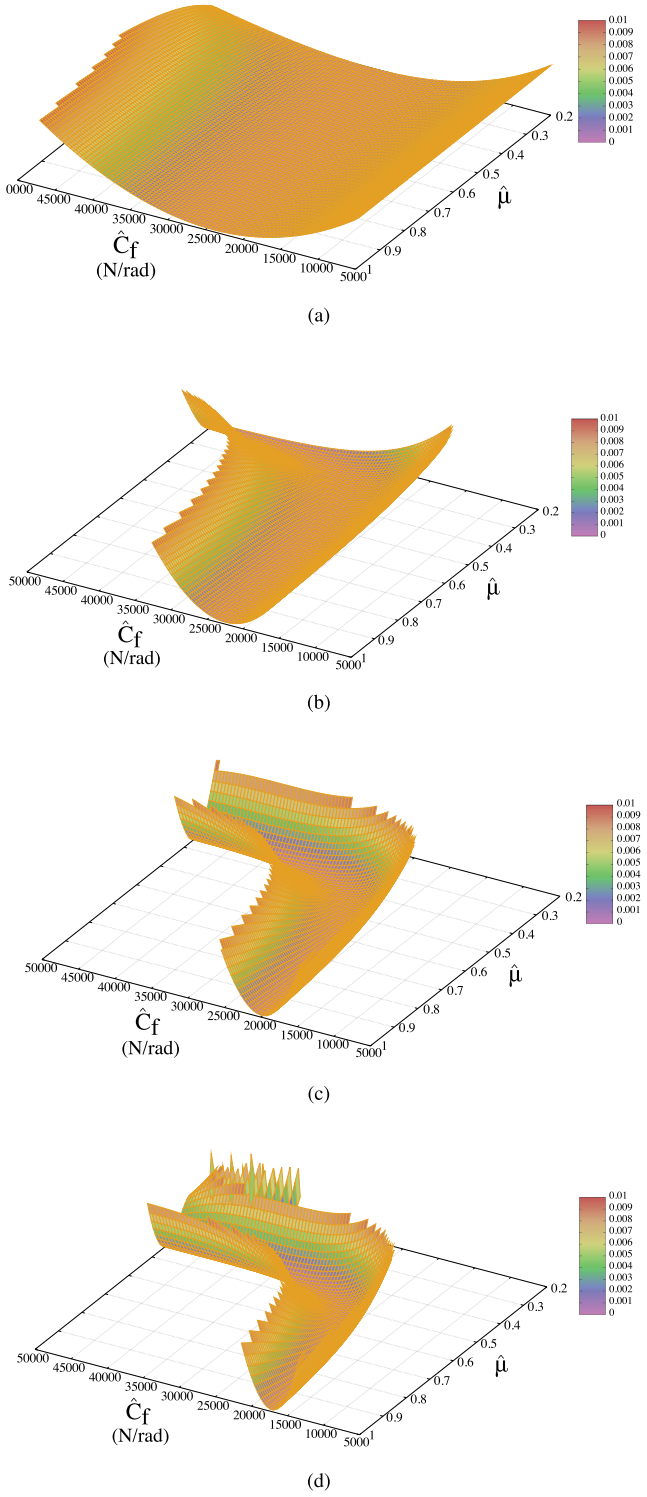

FIGURE 3. Square of the yaw rate error with respect to the estimated parameters ($\hat{\mu}$ and $\hat{C}_f$). Real parameters: $F_{zf} \equiv F_{zr} = 5000$ N, $\mu = 0.5$ and $C_f = 25000$ N/rad (a) $|\alpha_f| = 0.02$ rad (b) $|\alpha_f| = 0.05$ rad (c) $|\alpha_f| = 0.1$ rad (d) $|\alpha_f| = 0.15$ rad.

parameters are investigated to guarantee the convergence of the adaptive law in Fig. 4.

A direct analysis of the results presented in Fig. 4(a) shows that the convergence of the adaptive law exhibits different

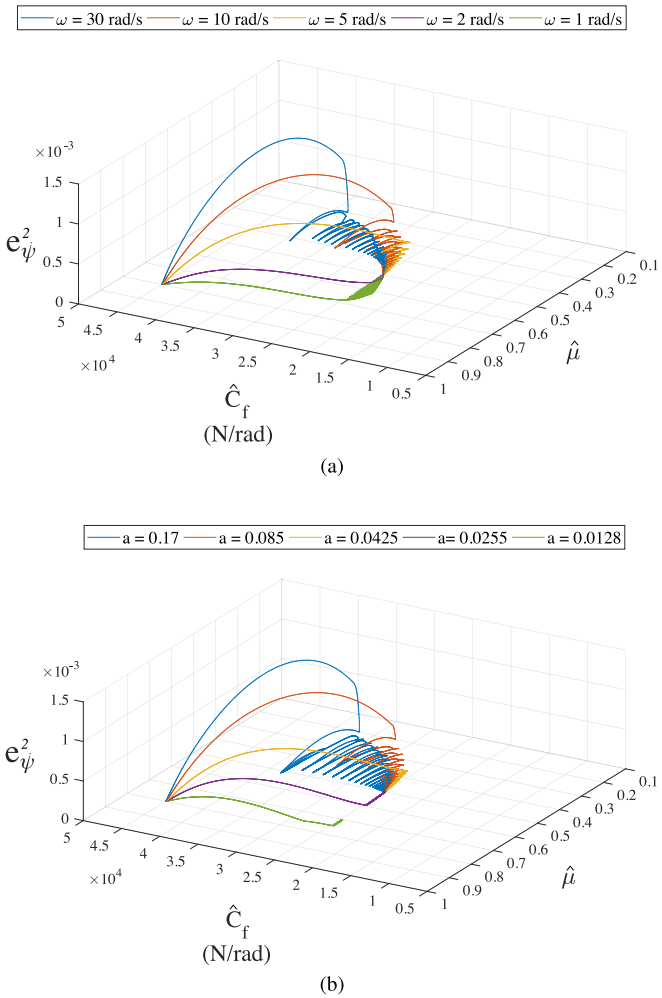

FIGURE 4. Adaptive law trajectory for the side slip angle functions: (a) $\alpha_f(t) = 0.085\sin(\omega t)$ (b) $\alpha_f(t) = a\sin(10t)$. Real parameters: $F_{zf} \equiv F_{zr} = 5000$ N, $\mu = 0.5$ and $C_f = 25000$ N/rad.

trajectories for different frequency values ω. Fig. 4(b) expresses the trajectory of the same adaptive law, but this time with different amplitude values a by fixing the frequency to $\omega = 10\,\text{rad}/s$. This last result clearly shows that the convergence of the parameters to the true values fails as the amplitude of the tire slip angle signal decreases. This behavior is expected as the system trajectory does not provide a distinguishable set, note that, for $a = 0.02$ the square of the yaw rate error will be defined by the function presented in Fig. 3(a) with respect to the estimated parameters. This function shows that the system would not be able to converge to the real parameters as any value $\hat{C}_f = 25000$ N/rad and $\hat{\mu} = x$ will be a global minimum.

To understand the effect of the observer gain l_1 into the adaptive algorithm we introduce the result of Fig. 5. As expected, by increasing the observer gain, the bursting effect becomes smaller and the state estimation error will converge more quickly, nonetheless, the parameters convergence time will increase.

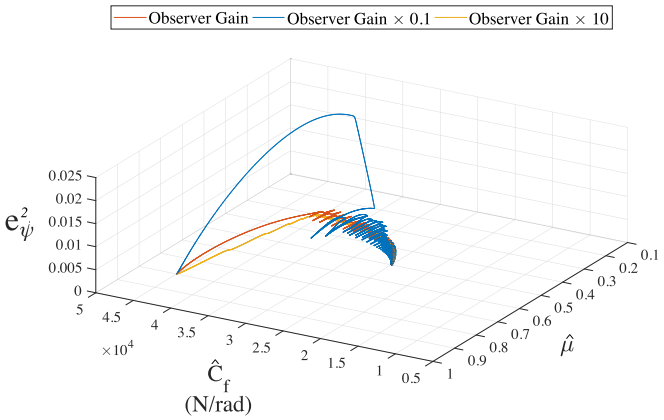

FIGURE 5. Effect of the observer gain on the bursting phenomena. Real parameters: $F_{zf} \equiv F_{zr} = 5000$ N, $\mu = 0.5$ and $C_f = 25000$ N/rad ($\alpha_f(t) = 0.085\sin(10t)$).

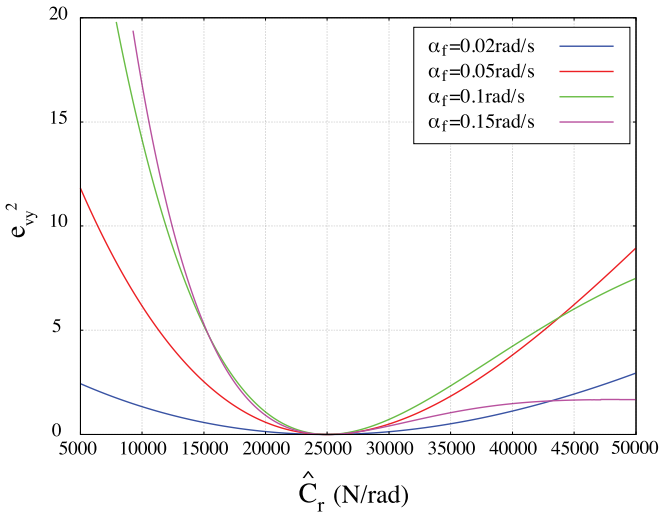

FIGURE 6. Square of the lateral velocity error with respect to the estimated parameter ($\hat{C}_r$). Real parameters: $F_{zf} \equiv F_{zr} = 5000$ N, $\mu = 0.5$ and $C_r = 25000$ N/rad.

Until this point, we have only consider the convergence of the first adaptive law defined in (15) with the projection strategy expressed by (21). We will now address the adaptive law defined by (20). In our analysis we will assume that the proposed trigger mechanism will only activate the adaptive law whenever the convergence of both $\hat{C}_f$ and $\hat{\mu}$ to its true values is attained.

Similarly to what was done in the first stage of the adaptive algorithm, the Lyapunov function in (16) will be pursued by analysing the square of the lateral velocity error with respect to the estimated variable $\hat{C}_r$. Note that we will consider that $\hat{\mu} \approx \mu$ in this scenario.

Fig. 6 expresses the square of the lateral velocity error with respect to the rear cornering stiffness estimation parameter. Fig. 6 allow us to further investigate the convexity characteristic for different tire slip angles of the rear tire. The analysis of the system in the conditions presented in Fig. 6 shows that the function is convex for small tire side slip angles, however, as this variable increases, this characteristic is lost. Nonetheless, a weaker condition of Lipschitz continuity of the gradient of the Lyapunov function is still valid for higher side slip angles, in the admissible set [33]. As a result, the second level of the proposed adaptive algorithm converges to the real value as long as the friction coefficient is correctly obtained by the first adaptive law.

TABLE 1. Class B: Vehicle Parameters (Carsim)

Description	Value	Units	Parameter
Mass of the vehicle	1110	$[kg]$	m
Yaw moment of inertia	1343	$[kg \cdot m^2]$	I_z
Distance of the front tire to CoG	1.04	$[m]$	l_f
Distance of the rear tire to CoG	1.56	$[m]$	l_r
Height of the CoG	0.54	$[m]$	h

V. RESULTS

The performance of the developed algorithm will be addressed in this section through computational simulation in Matlab/Simulink. The vehicle dynamic model is introduced by a high fidelity full order Carsim model, the parameters of the vehicle are presented in Table I. To ensure a realistic scenario, Gaussian sensor noise will be added to the output of the Carsim model.

A. IDENTIFICATION SOLUTION

The experiment will be designed to evaluate the performance of the identification algorithm developed in Section III. A total of four different scenarios will be presented to analyze the proposed algorithm in different driving and road conditions.

Two scenarios will be initially pursued: a high speed maneuver (varying from 90 km/h to 110 km/h), where the vehicle transits from a dry road ($\mu = 0.85$) to a wet surface ($\mu = 0.65$), hereafter called Scenario I, and a low speed maneuver (constant longitudinal velocity of 50 km/h) with lower friction conditions, hereafter called Scenario II. Furthermore, to evaluate the impact of different tire models in the proposed algorithm, we will present two tire data sets: tire A (Touring 185/65 R15) and tire B (Touring 215/55 R17).

In the first scenario, the vehicle will be equipped with type A tires, nonetheless, in the second scenario the front tires will be type A and the rear tires will be evaluated with both tires (A and B). These scenarios will allow us to evaluate the performance of the proposed algorithm for different road conditions and tire parameters.

A more realistic double lane change (DLC) scenario, hereafter called Scenario III, is also studied in this section. In this experiment, we will pursue a typical maneuver to evaluate the performance of the proposed solution in normal driving conditions without any constraints on the steering behavior, which will be controlled by a human driver simulator provided by CarSim tool. Like in the first scenario, the vehicle will be equipped with Touring 185/65 R15 tires (type A).

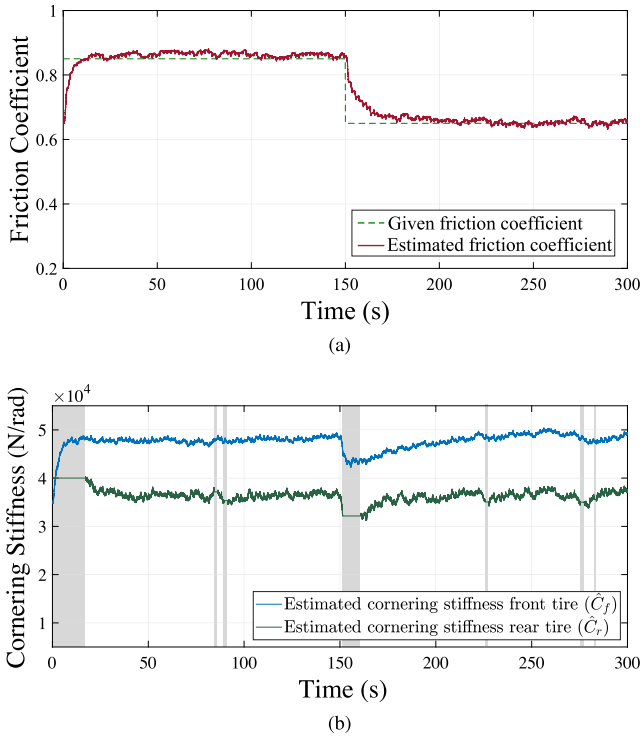

FIGURE 7. Scenario I - Evolution of the estimated parameters during a sinusoidal maneuver ($\delta = 0.06\sin(\pi/2t)$) (a) Tire-road friction coefficient ($\hat{\mu}$) (b) Cornering stiffness of the front and rear tire ($\hat{C}_f$ and $\hat{C}_r$ respectively).

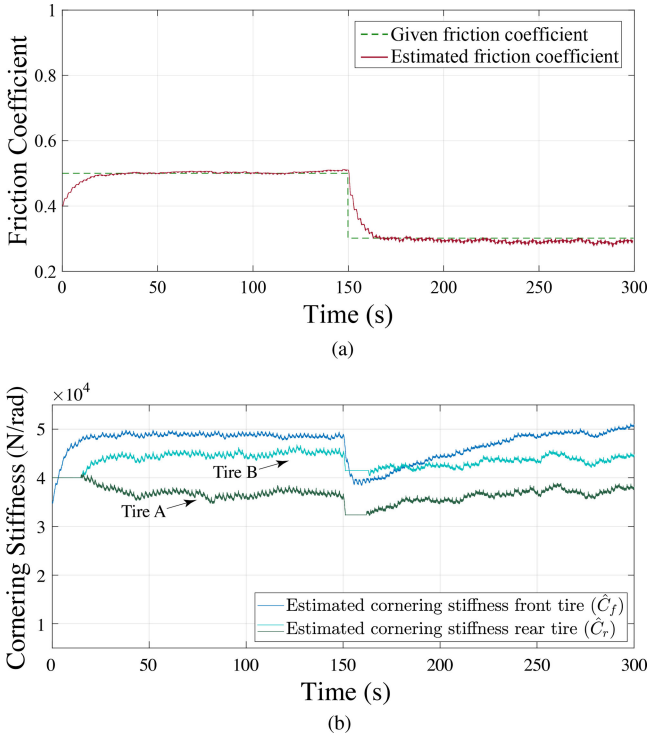

FIGURE 8. Scenario II - Evolution of the estimated parameters during a sinusoidal maneuver ($\delta = 0.08\sin(\pi/2t)$) (a) Tire-road friction coefficient ($\hat{\mu}$) (b) Cornering stiffness of the front and rear tire ($\hat{C}_f$ and $\hat{C}_r$ respectively).

Finally, we will analyze the friction coefficient estimation in the presence of an extremely varying road condition. To this end, the given friction coefficient will be defined as a constant value disturbed by a random quantity that will emulate a quickly varying friction condition, this will be defined as Scenario IV.

SCENARIO I

In this first scenario, the vehicle starts the maneuver at 100 km/h and follows a triangular reference, linearly increasing its velocity to 110 km/h in 10 s and then decelerates to 90 km/h after 20 s, this behavior is repeated for the duration of the experiment to evaluate the impact of the longitudinal dynamic in the developed algorithm.

A dynamic steering maneuver is pursued in this experiment by introducing a sinusoidal steering command ($a_\delta \sin(\omega_\delta t)$) to the vehicular system. The steering peak value will be establish at $a_\delta = 0.06$ rad and the frequency of the periodic signal will be defined as $\omega_\delta = \pi/2$ rad/s.

The estimated values of the proposed adaptive sequential algorithm are presented in Fig. 7. The tire-road friction coefficient is initially parameterized for a dry road scenario ($\mu = 0.85$), at time instant $t = 150$ s a sudden change in the friction coefficient is introduced, dropping the friction coefficient to $\mu = 0.65$, which corresponds to a typical wet road scenario [7].

The identification algorithm is able to correctly estimate the friction coefficient and cornering stiffness of both front and rear tires, even in the presence of longitudinal dynamic. As expected, the algorithm inhibit the second level of the adaptive law whenever the first layer is trying to converge. The inhibit period is depicted in Fig. 7(b) by a shaded area that indicates that the second adaptive law is disabled.

SCENARIO II

This experiment is designed to evaluate the performance of the proposed algorithm in more challenging road friction conditions. In this scenario, the vehicle follows at a constant longitudinal velocity of 50 km/h and, once again, a lateral excitation is imposed by introducing a sinusoidal steering command ($a_\delta \sin(\omega_\delta t)$) to the vehicular system. The vehicle will initially follow in a wet road with $\mu = 0.5$ and, at $t = 150$ s, the road conditions suddenly change to $\mu = 0.3$ (snowy conditions) [7]. The steering peak value will be defined as $a_\delta = 0.08$ rad and the frequency of the periodic signal will be $\omega_\delta = \pi/2$ rad/s.

The results presented in Fig. 8 have shown that the algorithm is able to obtain a correct estimation of the friction coefficient in challenging conditions. Even more, the two stage algorithm is capable of estimating both front and rear cornering stiffness for different tire data sets.

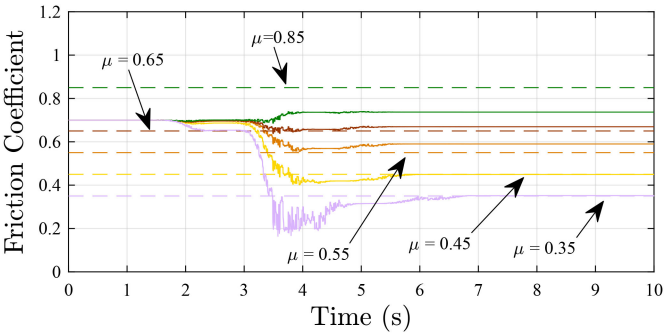

FIGURE 9. Scenario III - Estimation of the tire-road friction coefficient in a Double Lane Change maneuver for different road conditions.

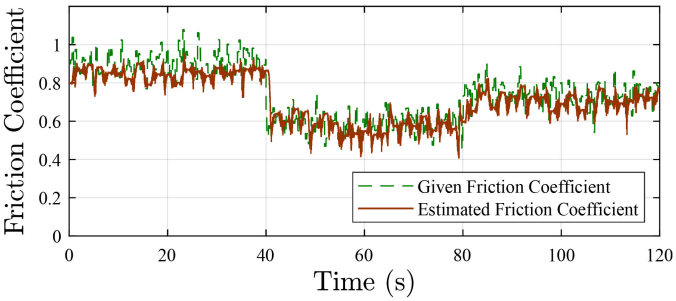

FIGURE 10. Scenario IV - Estimation of the tire-road friction coefficient in quickly varying road conditions.

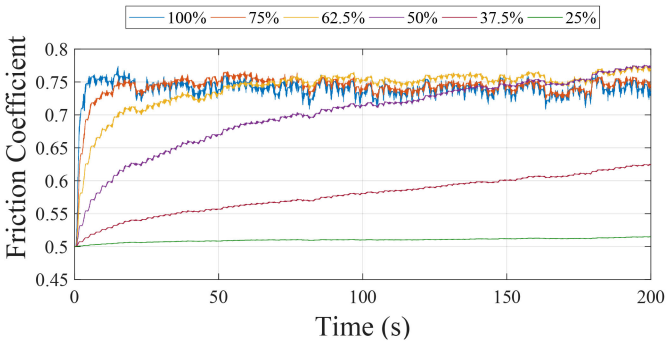

FIGURE 11. Estimation of the tire-road friction coefficient in the presence of different sinusoidal steering inputs: $\delta = a_\delta \sin(\pi/2t)$.

SCENARIO III

Contrary to the first two scenarios, this experiment will not impose a specific steering behavior to ensure persistent excitation of the system. This third scenario will present a typical double lane change maneuver with a closed-loop driver path follower model defined by CarSim tool. The vehicle's longitudinal velocity will be controlled at 120 km/s.

This scenario allows the evaluation of the identification procedure of the friction coefficient parameter in various road condition. The friction coefficient estimation results in a DLC maneuver are presented in Fig. 9.

From the analysis of the results depicted in Fig. 9 becomes clear that the algorithm is able to correctly estimate low friction coefficient conditions, nonetheless, as the road conditions become less slippery, the parameters are not able to converge to their true values.

In low friction conditions, the driver model present a more aggressive steering behavior to ensure the path following condition thus leading to high level of excitation ultimately resulting in a clear parameter estimation. As the road conditions improves the driver is able to complete a maneuver more easily without requiring such an aggressive steering input leading to a less excited system.

This procedure demonstrated the performance of the system in a more realistic scenario. As expected, whenever the driver behaviour imposes a more dynamic steering command the lateral excitation will increase, thus leading the estimated parameters to the correct values. However, if a less demanding maneuver is executed, the algorithm will fail to converge to the true parameters due to lack of excitation.

SCENARIO IV

Since the road conditions will, in general, have a more demanding and uncertain characteristic, we will now pursue an experiment that will aim to emulate this scenario. The vehicle's longitudinal velocity will be controlled at 100 km/s and an excited sinusoidal input will be introduced at steering input ($\delta = 0.08\sin(\pi/2t)$). The result of scenario IV is presented in Fig. 10.

The previous results show a fair performance of the proposed adaptive law for the friction coefficient estimation. Although, the algorithm is not able to closely follow the rapid variations of the road conditions, the proposed solution is able to maintain a stable estimation of the friction coefficient.

B. EXCITATION OF THE SYSTEM

In Section IV it was evaluated the trajectory of the estimation algorithm in different excitation conditions. In order to further extend this analysis, we will investigate the impact of the excitation amplitude on the convergence time of the proposed solution. In Fig. 11 we analyze the convergence velocity of the estimated friction coefficient with different excitation amplitude a_δ. To allow a straightforward comparison, the frequency of the steering input is fixed to $\omega_\delta = \pi/2\,\text{rad}/s$ and the excitation amplitude is set to different values where $a_\delta = 0.08\,\text{rad}$ is defined as 100% for the purpose of this experiment.

A careful analysis of Fig. 11 revels that the convergence rate of the first level of the adaptive identification algorithm is closely linked to the excitation introduced by the steering angle of the vehicle. Furthermore, it is clear that a low excitation in the system may lead to the convergence of the parameters to an incorrect value, which was already established by the results in Fig. 4(b).

C. ROBUSTNESS ANALYSIS

In order to evaluate the robustness of the identification algorithm with regards to the known parameters of the vehicle, we will further investigate the friction coefficient parameter in the presence of parametric model mismatch.

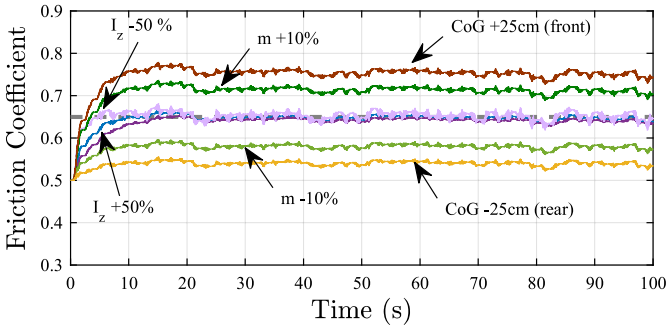

FIGURE 12. Estimation of the tire-road friction coefficient in the presence of model parametric mismatch.

To this end, it will be assumed a constant speed scenario (100 km/h) and a friction coefficient of $\mu = 0.65$ with a sinusoidal steering input $\delta = 0.08\sin(\pi/2t)$. The vehicle mass m, center of gravity CoG position and moment of inertial around the vertical axis I_z will be purposely altered to demonstrate the algorithm behavior in a poorly parameterized situation. The results are presented in Fig. 12.

The moment of inertia I_z has a minimum impact in the error of the estimation, however, it has a significant impact on the convergence speed of the algorithm which is to be expected since the adaptive law (15b) is inversely proportional to this parameter.

On the other hand, the mass and center of gravity of the vehicle introduces a bias to the estimation algorithm. This effect is also expected as the observer of the system relies on this parameters to produce the estimated states of the system. Note that, the lateral function of the front tire is defined as in (11), which is closely related to the vehicle mass and CoG, as a result, it is expected that the friction coefficient estimation may be affected by this mismatch. Thus we conclude that this algorithm is sensitive to mass changes and longitudinal shifts in the vehicle CoG.

To improve the robustness of this algorithm, the value of vehicle mass could be updated each time the vehicle initiates a new trip as suggested in similar frameworks presented in [4]. The vehicle CoG could also be estimated in real-time [34], thus ensuring the correct estimation of the friction coefficient.

VI. CONCLUSION

The presented work addresses the lateral dynamic identification problem for a ground vehicle system. Lyapunov based adaptive laws are proposed and a two stage sequential algorithm is developed. An estimation of the friction coefficient and the front tire cornering stiffness is obtained in the first level of the identification algorithm. Once the estimated values converge, the second level is trigger to estimate the rear tire cornering stiffness.

A graphical analysis of the Lyapunov function and the trajectory of the proposed adaptive laws were presented, allowing a more insightful discussion on the persistent excitation and the distinguishability properties. This investigation concluded that the convergence of the estimated variables to its true values can only be achieved if the system evolves to a set in which the only possible solution to this identification problem is the system's true parameters. To this end, a given lateral excitation must be assured to guarantee sufficient richness of the system, since, without this property it would be impossible to uniquely determine the cornering stiffness and tire-road friction coefficient.

To evaluate the performance of the proposed solution a computational simulation with a high fidelity vehicle model is pursued. The identification algorithm was able to correctly detect the system's true parameters, proving the good performance of the proposed solution for different driving condition.

ACKNOWLEDGMENT

The authors would like to thank Dr. Ricardo de Castro from German Aerospace Center (DLR) for his valuable comments and suggestions on this paper.

REFERENCES

[1] R. Rajamani, *Vehicle Dynamics and Control*. Berlin, Germany: Springer, 2011.
[2] J.-O. Hahn, R. Rajamani, and L. Alexander, "GPS-based real-time identification of tire-road friction coefficient," *IEEE Trans. Control Syst. Technol.*, vol. 10, no. 3, pp. 331–343, May 2002.
[3] R. Rajamani, N. Piyabongkarn, J. Lew, K. Yi, and G. Phanomchoeng, "Tire-road friction-coefficient estimation," *IEEE Control Syst. Mag.*, vol. 30, no. 4, pp. 54–69, Aug. 2010.
[4] R. Rajamani, G. Phanomchoeng, D. Piyabongkarn, and J. Y. Lew, "Algorithms for real-time estimation of individual wheel tire-road friction coefficients," *IEEE/ASME Trans. Mechatronics*, vol. 17, no. 6, pp. 1183–1195, Dec. 2012.
[5] M. Sharifzadeh, A. Senatore, A. Farnam, A. Akbari, and F. Timpone, "A real-time approach to robust identification of tyre–road friction characteristics on mixed-μ roads," *Vehicle Syst. Dyn.*, vol. 57, no. 9, pp. 1338–1362, 2019.
[6] Y.-W. Liao and F. Borrelli, "An adaptive approach to real-time estimation of vehicle sideslip, road bank angles, and sensor bias," *IEEE Trans. Veh. Technol.*, vol. 68, no. 8, pp. 7443–7454, Aug. 2019.
[7] A. J. Tuononen, M. Ovaska, and A. Niskanen, "Review on tire-road-friction potential estimation technologies," in *Proc. IAVSD Int. Symp. Dyn. Vehicles Roads Tracks*, 2019, pp. 1027–1032.
[8] X. Jin, G. Yin, and N. Chen, "Advanced estimation techniques for vehicle system dynamic state: A survey," *Sensors*, vol. 19, no. 19, 2019, Art. no. 4289.
[9] M. Tanelli, L. Piroddi, and S. M. Savaresi, "Real-time identification of tire–road friction conditions," *IET Control Theory Appl.*, vol. 3, no. 7, pp. 891–906, 2009.
[10] L. Li, K. Yang, G. Jia, X. Ran, J. Song, and Z.-Q. Han, "Comprehensive tire–road friction coefficient estimation based on signal fusion method under complex maneuvering operations," *Mech. Syst. Signal Process.*, vol. 56, pp. 259–276, 2015.
[11] D. Barbosa, A. Lopes, and R. E. Araújo, "Sensor fusion algorithm based on extended kalman filter for estimation of ground vehicle dynamics," in *Proc. IECON 2016-42nd Annu. Conf. IEEE Ind. Electron. Soc*, 2016, pp. 1049–1054.
[12] C. Ahn, H. Peng, and H. E. Tseng, "Robust estimation of road friction coefficient using lateral and longitudinal vehicle dynamics," *Veh. Syst. Dyn.*, vol. 50, no. 6, pp. 961–985, 2012.
[13] C. Ahn, H. Peng, and H. E. Tseng, "Robust estimation of road frictional coefficient," *IEEE Trans. Control Syst. Technol.*, vol. 21, no. 1, pp. 1–13, Jan. 2013.
[14] C. Lee, K. Hedrick, and K. Yi, "Real-time slip-based estimation of maximum tire-road friction coefficient," *IEEE/ASME Trans. Mechatronics*, vol. 9, no. 2, pp. 454–458, Jun. 2004.

[15] Y.-H. Liu, T. Li, Y.-Y. Yang, X.-W. Ji, and J. Wu, "Estimation of tire-road friction coefficient based on combined APF-IEKF and iteration algorithm," *Mech. Syst. Signal Process.*, vol. 88, pp. 25–35, 2017.
[16] K. Yi, K. Hedrick, and S.-C. Lee, "Estimation of tire-road friction using observer based identifiers," *Veh. Syst. Dyn.*, vol. 31, no. 4, pp. 233–261, 1999.
[17] M. Choi, J. J. Oh, and S. B. Choi, "Linearized recursive least squares methods for real-time identification of tire–road friction coefficient," *IEEE Trans. Veh. Technol.*, vol. 62, no. 7, pp. 2906–2918, Sep. 2013.
[18] J. Wang, L. Alexander, and R. Rajamani, "Friction estimation on highway vehicles using longitudinal measurements," *J. Dyn. Syst., Meas., Control*, vol. 126, no. 2, pp. 265–275, 2004.
[19] G. Erdogan, L. Alexander, and R. Rajamani, "Estimation of tire-road friction coefficient using a novel wireless piezoelectric tire sensor," *IEEE Sensors J.*, vol. 11, no. 2, pp. 267–279, Feb. 2010.
[20] S. Hong, G. Erdogan, K. Hedrick, and F. Borrelli, "Tyre–road friction coefficient estimation based on tyre sensors and lateral tyre deflection: Modelling, simulations and experiments," *Veh. Syst. Dyn.*, vol. 51, no. 5, pp. 627–647, 2013.
[21] L. Shao, C. Jin, C. Lex, and A. Eichberger, "Robust road friction estimation during vehicle steering," *Veh. Syst. Dyn.*, vol. 57, no. 4, pp. 493–519, 2019.
[22] R. Wang and J. Wang, "Tire–road friction coefficient and tire cornering stiffness estimation based on longitudinal tire force difference generation," *Control Eng. Pract.*, vol. 21, no. 1, pp. 65–75, 2013.
[23] R. N. Jazar, *Vehicle Dynamics: Theory and Application.* Berlin, Germanu: Springer, 2008.
[24] A.-P. Loh, A. M. Annaswamy, and F. P. Skantze, "Adaptation in the presence of a general nonlinear parameterization: An error model approach," *IEEE Trans. Autom. Control*, vol. 44, no. 9, pp. 1634–1652, Sep. 1999.
[25] K. Narendra, I. Khalifa, and A. Annaswamy, "Error models for stable hybrid adaptive systems," *IEEE Trans. Autom. Control*, vol. 30, no. 4, pp. 339–347, Apr. 1985.
[26] P. A. Ioannou and J. Sun, *Robust Adaptive Control*. Mineola, New York, NY, USA: Courier Corporation, 2012.
[27] L. Hsu and R. Costa, "Bursting phenomena in continuous-time adaptive systems with a σ-modification," *IEEE Trans. Autom. Control*, vol. 32, no. 1, pp. 84–86, Jan. 1987.
[28] A. M. Annaswamy, F. P. Skantze, and A.-P. Loh, "Adaptive control of continuous time systems with convex/concave parametrization," *Automatica*, vol. 34, no. 1, pp. 33–49, 1998.
[29] K. S. Narendra and A. M. Annaswamy, "Persistent excitation in adaptive systems," *Int. J. Control*, vol. 45, no. 1, pp. 127–160, 1987.
[30] P. A. Ioannou and G. Tao, "Dominant richness and improvement of performance of robust adaptive control," *Automatica*, vol. 25, no. 2, pp. 287–291, 1989.
[31] R. Hermann and A. Krener, "Nonlinear controllability and observability," *IEEE Trans. Autom. Control*, vol. 22, no. 5, pp. 728–740, Oct. 1977.
[32] L. Lennart, *System Identification: Theory for the User. Upper Saddle River, NJ, USA: Prentice-Hall*, 1999, pp. 1–14.
[33] H. H. Bauschke, J. Bolte, J. Chen, M. Teboulle, and X. Wang, "On linear convergence of Non-Euclidean gradient methods without strong convexity and lipschitz gradient continuity," *J. Optim. Theory Appl.*, vol. 182, no. 3, pp. 1068–1087, 2019.
[34] J. Lee, D. Hyun, K. Han, and S. Choi, "Real-time longitudinal location estimation of vehicle center of gravity," *Int. J. Autom. Technol.*, vol. 19, no. 4, pp. 651–658, 2018.

ANTÓNIO LOPES (Student Member, IEEE) was born in Portugal, in 1991. He received the M.S. degree in electrical and computer engineering from the Faculty of Engineering, University of Porto, Porto, Portugal, in 2014.

From 2014 to 2015 he was a Researcher in PT Inovação in Aveiro, Portugal. Since 2015 he has been working as a Researcher in the Smart Grids and Electric Vehicles Laboratory in the Institute for Systems and Computer Engineering, Technology and Science (INESC TEC), in Porto, Portugal. He has developed work in power electronic and control systems and has been involved in European research projects in the area of smart grids and electric vehicles. He is currently working towards the Ph.D. degree in electrical and computer engineering at the Faculty of Engineering, University of Porto. His research interests include vehicle dynamics, platooning, control and decision, fault tolerant control, fault diagnosis and power electronics systems.

RUI ESTEVES ARAÚJO (Member, IEEE) received the Electrical Engineering diploma, and the M.Sc. and Ph.D. degrees from the University of Porto, Porto, Portugal, in 1987, 1992, and 2001, respectively. From 1987 to 1988, he was an Electrotechnical Engineer in the Project Department, Adira Company, Porto, Portugal, and from 1988 to 1989, he was a Researcher in the Institute for Systems and Computer Engineering (INESC), Porto, Portugal. Since 1989, he has been with the University of Porto, where he is currently an Assistant Professor in the Department of Electrical and Computer Engineering, Faculty of Engineering, University of Porto. He is a Senior Researcher in the INESC Technology and Science, focusing on control theory and its industrial applications to motion control, electric vehicles, and renewable energies.